Pharmacophore-based discovery of FXR-agonists. Part II: Identification of bioactive triterpenes from *Ganoderma lucidum*

Ulrike Grienke [a], Judit Mihály-Bison [b], Daniela Schuster [c], Taras Afonyushkin [b], Markus Binder [b], Shu-hong Guan [d], Chun-ru Cheng [d], Gerhard Wolber [e], Hermann Stuppner [a], De-an Guo [d], Valery N. Bochkov [b], Judith M. Rollinger [a,*]

[a] *Institute of Pharmacy/Pharmacognosy and Center for Molecular Biosciences Innsbruck, University of Innsbruck, Innrain 52c, 6020 Innsbruck, Austria*
[b] *Center of Biomolecular Medicine and Pharmacology, Department of Vascular Biology and Thrombosis Research, Medical University of Vienna, Schwarzspanierstraße 17, 1090 Vienna, Austria*
[c] *Computer-Aided Molecular Design Group, Institute of Pharmacy/Pharmaceutical Chemistry and Center for Molecular Biosciences Innsbruck, University of Innsbruck, Innrain 52c, 6020 Innsbruck, Austria*
[d] *Shanghai Institute of Materia Medica, Chinese Academy of Sciences, 555 Zu Chong Zhi Road, Zhang Jiang Hi-Tech Park, Pudong, 201203 Shanghai, China*
[e] *Institute of Pharmacy/Pharmaceutical Chemistry, Freie Universität Berlin, Königin-Luise-Str. 2+4, 14195 Berlin, Germany*

ARTICLE INFO

ABSTRACT

The farnesoid X receptor (FXR) belonging to the metabolic subfamily of nuclear receptors is a ligand-induced transcriptional activator. Its central function is the physiological maintenance of bile acid homeostasis including the regulation of glucose and lipid metabolism. Accessible structural information about its ligand-binding domain renders FXR an attractive target for in silico approaches. Integrated to natural product research these computational tools assist to find novel bioactive compounds showing beneficial effects in prevention and treatment of, for example, the metabolic syndrome, dyslipidemia, atherosclerosis, and type 2 diabetes. Virtual screening experiments of our in-house Chinese Herbal Medicine database with structure-based pharmacophore models, previously generated and validated, revealed mainly lanostane-type triterpenes of the TCM fungus *Ganoderma lucidum* Karst. as putative FXR ligands. To verify the prediction of the in silico approach, two *Ganoderma* fruit body extracts and compounds isolated thereof were pharmacologically investigated. Pronounced FXR-inducing effects were observed for the extracts at a concentration of 100 μg/mL. Intriguingly, five lanostanes out of 25 secondary metabolites from *G. lucidum*, that is, ergosterol peroxide (**2**), lucidumol A (**11**), ganoderic acid TR (**12**), ganodermanontriol (**13**), and ganoderiol F (**14**), dose-dependently induced FXR in the low micromolar range in a reporter gene assay. To rationalize the binding interactions, additional pharmacophore profiling and molecular docking studies were performed, which allowed establishing a first structure–activity relationship of the investigated triterpenes.

1. Introduction

Farnesoid X receptor (FXR; NR1H4), a ligand-induced transcriptional activator is a member of the nuclear hormone receptor superfamily.[1] It is expressed in liver, intestine, kidney, adrenal glands, and also in the vasculature where FXR might play a role in the pathogenesis of cardiovascular diseases.[1,2]

FXR, like other nuclear receptors, comprises a variable modular region, a conserved DNA binding domain (DBD) and a ligand binding domain (LBD).[3] It acts as monomer (e.g., stimulating the expression of the main insulin-responsive glucose transporter GLUT4), as homodimer, or preferentially with its partner the nuclear receptor 9-*cis*-retionic acid receptor (RXR), forming an FXR/RXR-heterodimer.[3,4] Upon ligand binding, the receptor connects to DNA which results either in an up-regulation or repression of gene transcription.[3] The resulting mechanisms are influenced by the agonist or antagonist character of the respective ligand.[3]

In 1999, FXR has been found to be a key target for bile acids (BAs).[5–7] Representing endogenous signaling molecules, BAs negatively regulate their own synthesis by repressing the transcription of cholesterol 7α-hydroxylase (CYP7A1), a cytochrome P450 enzyme essential for the synthesis of cholesterol. This mechanism

involves the small heterodimer partner 1 (SHP-1), a nuclear receptor without DBD.[8,9]

Among others, genes encoding the intestinal bile acid-binding protein (IBABP) and the bile salt export pump (BSEP) are also regulated via FXR activation.[5,10,11] The involved mechanisms are important for BA secretion and transportation.

Besides cholic acid (CA), deoxycholic acid (DCA) and lithocholic acid (LCA), the primary BA chenodeoxycholic acid (CDCA) represents the most potent endogenous FXR ligand with EC_{50} values between 10 and 50 μM (Chart 1).[3,5–7] For a pharmacological characterization and evaluation of the drugability of FXR, several synthetic ligands have been developed. These can be categorized in steroids (Chart 1), like, for example, 6-ethylchenodeoxycholic acid (6-ECDCA; INT-747),[12] and non steroids (Chart 2), like, for example, GW4064,[13] AGN29,[14] and AGN31.[14]

For the identification of steroidal FXR ligands, derivatives of BAs have been developed to explore their structure–activity relationships. The thereby discovered most potent orally administered steroidal FXR agonist 6-ECDCA (INT-747)[12] (Chart 1) could already enter clinical studies for type 2 diabetes mellitus with presumed nonalcoholic fatty liver disease (NAFLD) and primary biliary cirrhosis (PBC).[15] Further clinical trials include the steroidal FXR ligands CDCA, and ursodeoxycholic acid (UDCA) (Chart 1).[15]

Among non-steroidal FXR agonists, especially GW4064 (Chart 2) has been studied intensively. Using this potent FXR agonist as lead structure, efforts to overcome shortcomings, that is, limited oral exposure, short terminal half-life, potential toxicity of the stilbene moiety, and UV light instability have been undertaken by various research groups. Analogues of GW4064 were synthesized by replacing the stilbene by naphthalene or benzothiophene rings which however in most cases did not result in improved FXR potency.[16,17] Current approaches led to the generation of more

effective GW4064 analogues by replacing the stilbene double bond by an oxymethylene or amino-methylene linker connecting a terminal benzoic acid with a substituted heteroaryl in the middle ring position.[18]

Aside from mentioned GW4064 analogues, high-throughput screening campaigns revealed benzimidazole derivatives and azepino(4,5-b)indole derivatives as new classes of FXR agonists.[19]

WAY-362450 (Chart 2), a representative of the latter group, was investigated in the course of clinical trials in healthy subjects to validate the safety, tolerability, and pharmacokinetics of this orally administered FXR agonist.[20]

In recent publications the relevance of FXR as BA activated receptor was illuminated with regard to the treatment of atherosclerosis and its counter-regulatory role in immunity and inflammation.[21,22] Beneficial effects of FXR agonists are reported for the modulation of lipids[23] and glucose as well as hepatobiliary and gastrointestinal diseases.[24]

On the one hand FXR holds a regulative function in many endogenous pathways and on the other hand the features of its active site are well-characterized.[25,26] These essential facts contribute to the attractiveness of this nuclear receptor as novel drugable target to find innovative agents showing favorable effects in the prevention and treatment of, for example, the metabolic syndrome, dyslipidemia, atherosclerosis, and type 2 diabetes.[25,26]

Especially in recent years natural products regulating nuclear receptors have been found to play an important role as promising candidates in drug development.[27] Concerning the nuclear receptor FXR, the most investigated ones are the stereoisomeres *E*- and *Z*-guggulsterone (Chart 3), the bioactive constituents of the stem bark resin of *Commiphora mukul* (Burseraceae), which is used in Ayurvedic medicine for the treatment of lipid disorders and
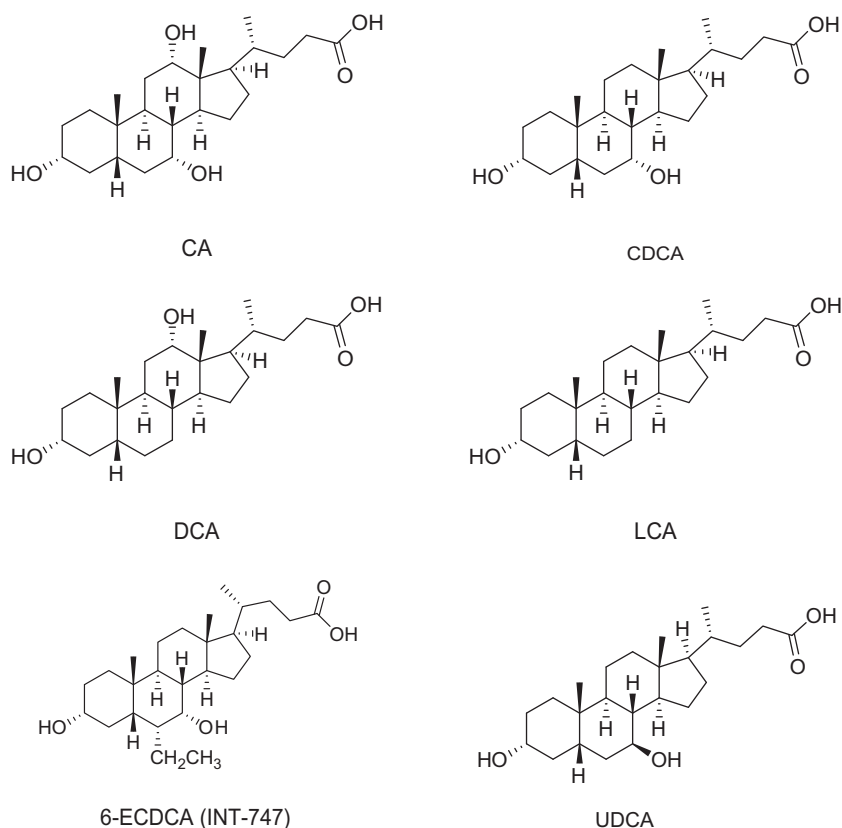

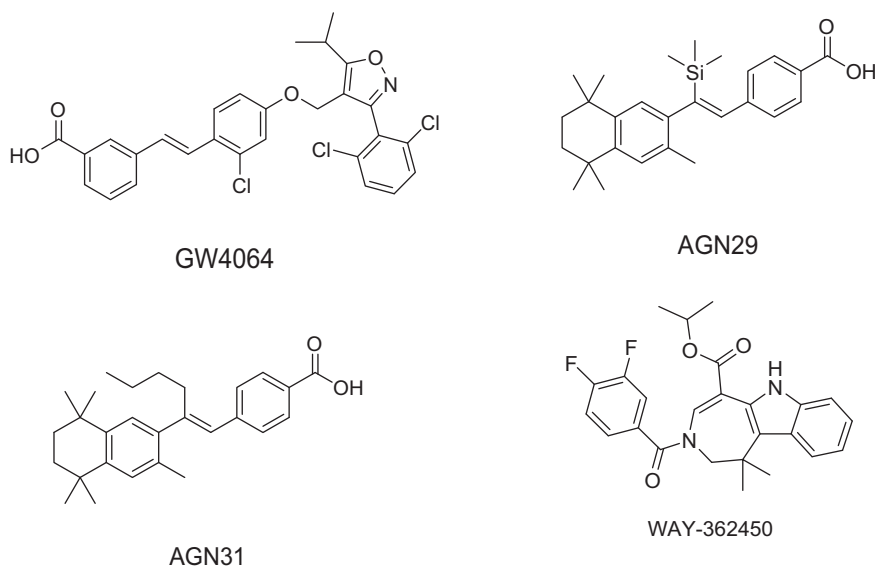Chart 1. Examples of chemical structures of steroidal FXR ligands.

GW4064

AGN29

AGN31

WAY-362450

Chart 2. Examples of chemical structures of non-steroidal FXR ligands.

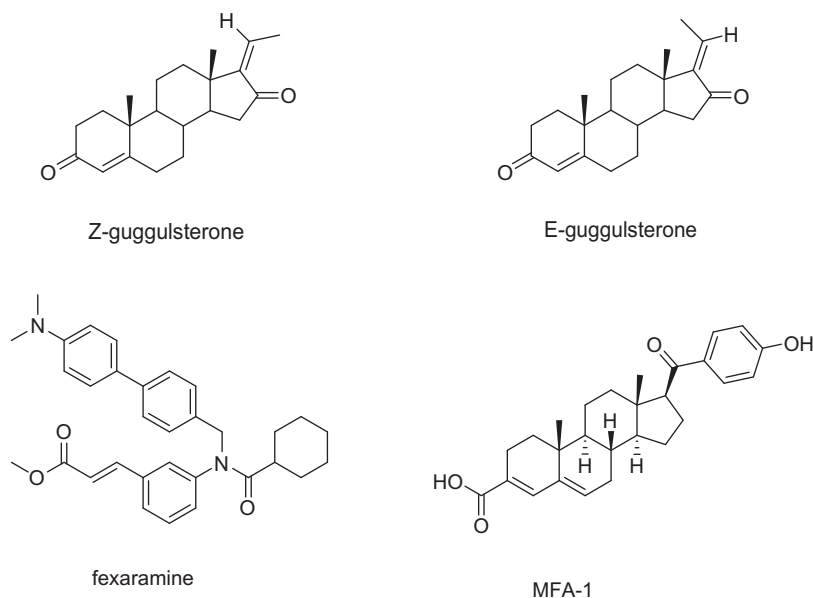
Z-guggulsterone

E-guggulsterone

fexaramine

MFA-1

Chart 3. Chemical structures of stereoisomeres Z- and E-guggulsterone, fexaramine (y-shaped synthetic FXR agonist used for co-crystallization with human FXR as reported in the PDB entry 1osh), and MFA-1 (synthetic FXR agonist used for co-crystallization with human FXR as reported in the PDB entry 3bej).

obesity.[28] The pregnane derivatives E- and Z-guggulsterone, as observed in a mouse model, act as FXR antagonists, which regulate the expression of a subset of targetgenes.[29] Efforts to discover the mode of action of these cholesterol-lowering compounds revealed an FXR-antagonism by suppressing the expression of BSEP and upregulating CYP7A1. However, this mechanism is combined with the ability to dominantly enhance the transactivation of BSEP, thus indirectly leading to an FXR-agonistic effect.[30]

Several studies report also an interaction of E- and Z-guggulsterone with additional nuclear receptors such as, for example, the androgen receptor (AR), estrogen receptor (ERα), glucocorticosteroid receptor (GR), mineralcorticoid receptor (MR), progesterone receptor (PR), and the pregnane X receptor (PXR).[31,32] Furthermore, guggulsterone inhibits iNOS and COX-2 gene expressions, a mechanism which is suggested to involve the inhibition of NF-κB activation.[33]

An FXR-antagonism is postulated for scalarane-based sesterterpenes isolated from a marine sponge of the genus Spongia.[34] Xanthohumol, a prenylated chalcone, derived from Humulus lupulus (Cannabaceae) and extracts of the two traditional Chinese herbs Salvia miltiorrhiza (Lamiaceae) and Panax notoginseng (Araliaceae) are examples demonstrating FXR-inducing activity.[35–37]

The fruiting body of Ganoderma lucidum Karst. (reishi in Japan or língzhī in China), of the Ganodermataceae family, has been widely used in Asian traditional medicines for more than 2000 years. Many studies about the constituents of this medicinal mushroom have indicated antitumor, immunostimulating, anti-diabetic, anti-inflammatory, antiviral, antibacterial, antihypertensive, and hypolipidemic activities.[38] The pronounced pharmacological effects are mainly caused by triterpenes and polysaccharides. Over 200 triterpenes, mostly defined by an unsaturated lanostane scaffold, have been isolated from G. lucidum and the genus Ganoderma.[39] Due to the broad

6782

U. Grienke et al. / Bioorg. Med. Chem. 19 (2011) 6779–6791

spectrum of pharmacological effects related to *G. lucidum* and the vast number of involved constituents, an exact mechanism of action has only been assigned to a few compounds.

In this study we demonstrate the application of in silico tools for the identification of natural products, namely *Ganoderma* lanostane-type triterpenes as potent FXR agonists. These results might be in close relation to the known hypolipidemic and anti-inflammatory effects of the investigated medicinal fungus.

2. Results and discussion

For the identification of FXR ligands from natural sources we selected a virtual screening approach. Based on the protein data bank (PDB)[40] crystal structure entry 1osh[41] comprising a y-shaped hydrophobic ligand (Chart 3) within the binding site of the nuclear receptor FXR, a structure-based pharmacophore model (1osh-1) was created and validated in part I of this study.[42] The generated model consists of five hydrophobic features, one hydrogen bond acceptor with His294, and 27 exclusion volume spheres (Fig. 1).

Virtual screening of our in-house Chinese Herbal Medicine (CHM) database,[43] comprising 10,216 compounds, with the 1osh-1 model resulted in a list of 572 virtual hits (VHs) ranked according to their computationally derived best fit values. The analysis of the VHs comprising various compound classes involved several parameters, for example, already known FXR-related effects, commercial availability of the natural starting material or the pure compound, and accessibility of the selected VHs from natural sources. Considering these aspects a set of representatives has been selected for pharmacological evaluation of the predicted FXR-inducing potential taking into account diverse structure classes such as triterpenes, flavonoids, furanocoumarins, quinolone derivatives, carotenoids, and fatty acid derivatives. The selected VHs were found to be constituents of the fruit bodies of *G. lucidum* (GL), *Ginkgo biloba* (GB) leaves, *Vitex agnus-castus* (VAC) fruits, *Ruta graveolens* (RG) roots and leaves, *Capsicum annum* (CA) fruits, or *Panax ginseng* (PG) roots (Table 1).

To validate the in silico predictions extracts of different polarity (D = DCM; M = MeOH), an enriched ethyl acetate (EA) fraction, and available pure compounds (artemisetin, dihydrocapsaicin, and rutamarin) were screened for their FXR inducing potential in a reporter gene assay. The pharmacological evaluation of these substances was performed in HEK293 cells transiently transfected with the FXR reporter assay system comprising the ECRE-Luc reporter plasmid containing quintuple RXR:FXR binding site and the respective expression plasmids for full length murine FXR and RXRα. Correction for transfection efficiency of each sample was ensured by normalization of the firefly luciferase values to renilla luciferase that was co-transfected into the system (Fig. 2).

As reference, the effect of the well characterized FXR ligand CDCA (25 μM) versus untreated control was considered 100%, meaning a significant ($p < 0.001$, ANOVA, Bonferroni post-test) activation of the system. In comparison, at a test concentration of 100 μg/mL, the extracts of the fungus *G. lucidum* (GL_D and GL_M) induced FXR by about 150%, which, however, was not significantly different from the effect of CDCA. Furthermore, the ethyl acetate fraction of *V. agnus-castus* (VAC_EA) stimulated the nuclear receptor by 110.0%. All other tested extracts induced FXR to a lower percentage than the positive control CDCA. Among the pure compounds, artemisetin (10 μg/mL; 26 μM) and rutamarin (10 μg/mL; 28 μM) activated FXR significantly, but at lower extent than CDCA. No activation was observed with dihydrocapsaicin (10 μg/mL; 33 μM).

The data in Figure 2 identify the fruiting bodies of *G. lucidum* as promising starting material to scrutinize the active principles responsible for the observed FXR inducing effect. As the majority of already known constituents and all the VHs predicted from *Ganoderma* belong to the structural class of triterpenoids, respectively steroids, we decided to use a recently developed pharmacophore model[42] based on the PDB entry 3bej (co-crystallized with MFA-1)[44] which represents the structural class of steroids as active constituents (Chart 3). This pharmacophore model (3bej-1-s) consists of three hydrophobic features, two hydrogen bond acceptors anchoring the ligand with His294 and Thr288, a negatively ionizable feature representing the interaction with Arg331, and 25 exclusion volume spheres as well as a shape constraint for steric constraints to increase restrictivity (Fig. 3).[42] We expected this model to better represent steroidal compounds and lead to more triterpenoid hits in the database search. Accordingly, 3bej-1-s was then used to virtually screen the CHM database.

Due to the high restrictiveness of this structure-based pharmacophore model, which focuses on steroid-like compounds, only ten out of 10,216 structures could map the set features of the model (hit rate 0.098%). Interestingly, five of these VHs, namely four ganoderic acids and one lucidenic acid (Chart 4), are rare, but characteristic secondary metabolites from *G. lucidum*. Both types of these triterpenes are described by an unsaturated lanostane scaffold with a double bond in position 8 which is in conjugation with one to two oxo groups in positions 7 and 11. Ganoderic acids possess a carboxyl group in position 26 distinguishable from lucidenic acids with a decreased length of the side chain and a carboxyl group in position 24 (Chart 4).

Intriguingly, the used pharmacophore models, that is, 1osh-1 and 3bej-1-s, have been derived from ligands with unrelated chemical structures, both are able to find steroid-like compounds. Due to the differing model architecture of 1osh-1 and 3bej-1-s, the models did not retrieve identical steroidal hits from the CHM database. Anyway, both hit lists suggested lanostane-type triterpenes as potential FXR ligands. The CHM database used for virtual screening does not exhaustively cover all currently known TCM constituents.

As a consequence of the promising FXR-inducing effects determined for the *Ganoderma* extracts, and not to neglect further possibly bioactive compounds, we focused on the evaluation of all accessible pure constituents from the fruit body of *G. lucidum*.

Accordingly, 25 previously isolated *Ganoderma* constituents[45,46] were tested for their ability to induce FXR (Chart 5). Except for three fatty acid derivatives (**5–7**), they belong to the lanostane-type triterpenes, which can further be grouped into ergosterol
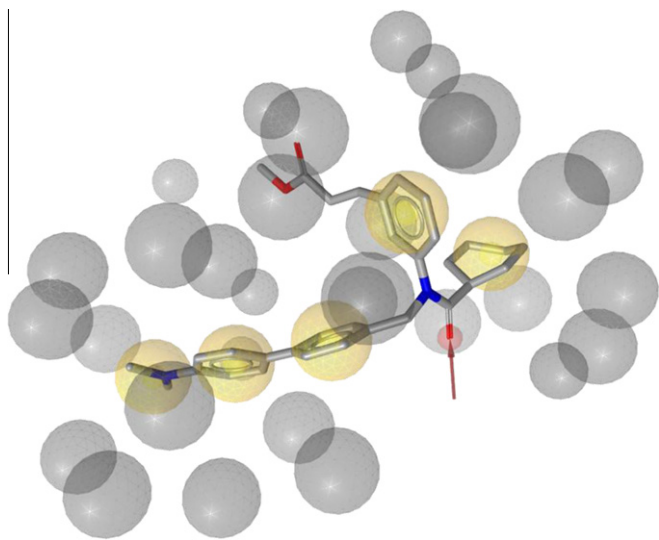

Figure 1. 1osh-1 Pharmacophore model comprising five hydrophobic features, one hydrogen bond acceptor with His294, and 27 exclusion volume spheres (ligand: fexaramine).

Table 1
Selected FXR-inducing VHs and respective natural sources predicted by the 1osh-1 pharmacophore model

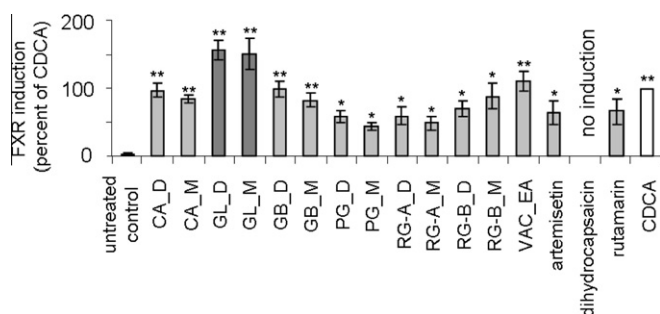| *Capsicum annuum* [fruit]	*Ganoderma lucidum* [fruit body]	*Ginkgo biloba* [leave]	*Panax ginseng* [root]	*Ruta graveolens* [root; herb]	*Vitex agnus-castus* [fruit]
Dihydrocapsaicin	Ganoderic acid α	Ginnol	*trans*-9,*trans*-12-Linoleic acid	Rotenone	Eupatorin
Nordihydrocapsaicin	Methyl ganoderate I	Hydroginkgolinic acid	*cis*-9,*cis*-12-Linoleic acid	Rutamarin	5-Hydroxy-3,6,7,4'-tetramethoxyflavone
Capsanthin	Ganoderic acid Z	Cardanol	Isooleic acid	1-Methyl-2-undecyl-4(1*H*)-quinolone	Casticin
	Ganoderic acid Y	*cis*-9,*cis*-12-Linoleic acid	3-Oxopanaxydol		Artemisetin
		Ginkgolic acid			
		Anacardic acid D			
		(+)-Catechin-pentaacetate			

Figure 2. Induction of FXR by DCM (D) and MeOH (M) extracts, one ethyl acetate (EA) fraction from different species as well as three pure compounds selected from the VH list of the 1osh-1 pharmacophore model tested in reporter gene assay. Activation of FXR-driven luciferase reporter in transfected cells was analyzed as described in the experimental section. The data (mean values ± SEM, $n = 4$–8) were normalized for renilla luciferase activity. The results are expressed as the difference in firefly luciferase activity between control and stimulated cells, normalized to the effect of positive control (CDCA, 25 μM); ($n = 7$–10; working concentration: extracts and fraction: 100 μg/mL, pure compounds: 10 μg/mL); (**$p < 0.01$, *$p < 0.05$, ANOVA, Bonferroni post-test)

Figure 3. 3bej-1-s Pharmacophore model with shape comprising three hydrophobic features, two hydrogen bond acceptors anchoring the ligand with His294 and Thr288, a negatively ionizable feature representing the interaction with Arg331, and 25 exclusion volume spheres (ligand: MFA-1).

derivatives (**1**, **2**, **4**), lanostanes with double bonds between the positions 7/8 and 9/11 (**3**, **9**, **12**–**14**), and lanostanes with a double bond between position 8/9 (**8**, **10**, **11**, **15**–**25**).

The selected compounds were tested in a reporter gene assay for FXR activation (Fig. 4). The cells were treated with the *Ganoderma* compounds or the positive control CDCA (25 μM). At a test concentration of 10 μM, the effect of seven *Ganoderma* constituents reached statistical significance, that is, **2**, **12**, **13**, **14**, **20** ($p < 0.001$) and **11**, **25** ($p < 0.01$).

A dose-dependent FXR-inducing activity could be confirmed for five of these lanostanes, namely for **2**, **11**, **12**, **13**, and **14** (Fig. 5) with EC$_{50}$ values of 0.85 μM (**2**), 2.5 μM (**13**), and 5.0 μM (**14**). Because no maximum effect has been reached by compounds **11** and **12** (test concentrations between 0.1 and 50 μM) the half maximal effective concentrations are estimated above 18.6 μM and 14.0 μM, respectively. For CDCA, an EC$_{50}$ of 16.8 μM was determined which is in agreement with previously published EC$_{50}$ values for CDCA.[3] Thus, the most active lanostanes identified from *G. lucidum*, that is, ergosterol peroxide (**2**), ganodermanontriol (**13**), and ganoderiol F (**14**) activated FXR at even lower concentrations than CDCA.

In order to obtain an independent evidence of the ability of the five lanostane-type triterpenes to activate FXR, we tested their effects on th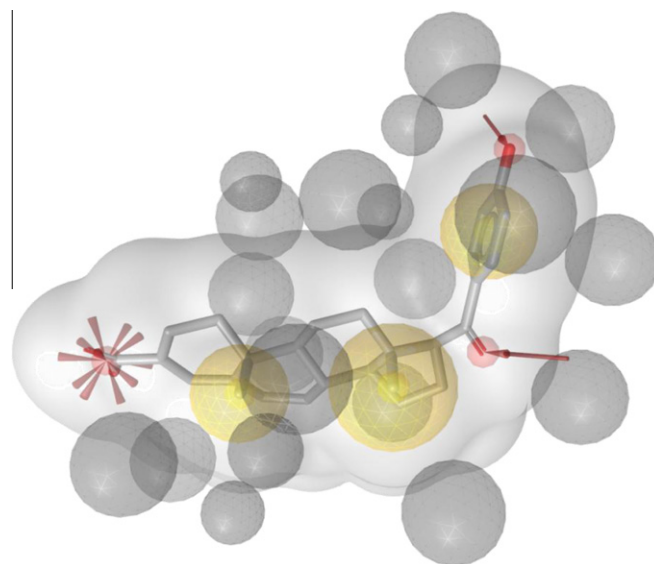e expression of a gene known to be downstream of FXR. CYP7A1 expression is down-regulated by FXR via a well-characterized molecular mechanism involving SHP and LRH-1, and is widely used to monitor activity of endogenously expressed FXR.[9] In full agreement with our promoter–reporter data, the five tested *Ganoderma* compounds significantly decreased the levels of CYP7A1 mRNA. The degree of inhibition was similar to that induced by the positive control CDCA (Fig. 6).

Compounds **2**, and **11**–**14** were further tested for anti-inflammatory effects. At a test concentration of 5 μM, these FXR-inducing compounds also prominently inhibited the TNF or LPS induced expression of IL-8 (Fig. 7A and B) and *E*-selectin (Fig. 7C and D) in human endothelial cells. These effects are comparable with the NFκB pathway inhibitor BAY-11-7085 at equimolar concentrations (5 μM). The observed FXR induction indicates a possible involvement of this nuclear receptor in the mechanism of the inflammatory regulation by these compounds.

In an attempt to identify the most appropriate model for triterpenoid FXR modulators, 13 pharmacophore models, generated and
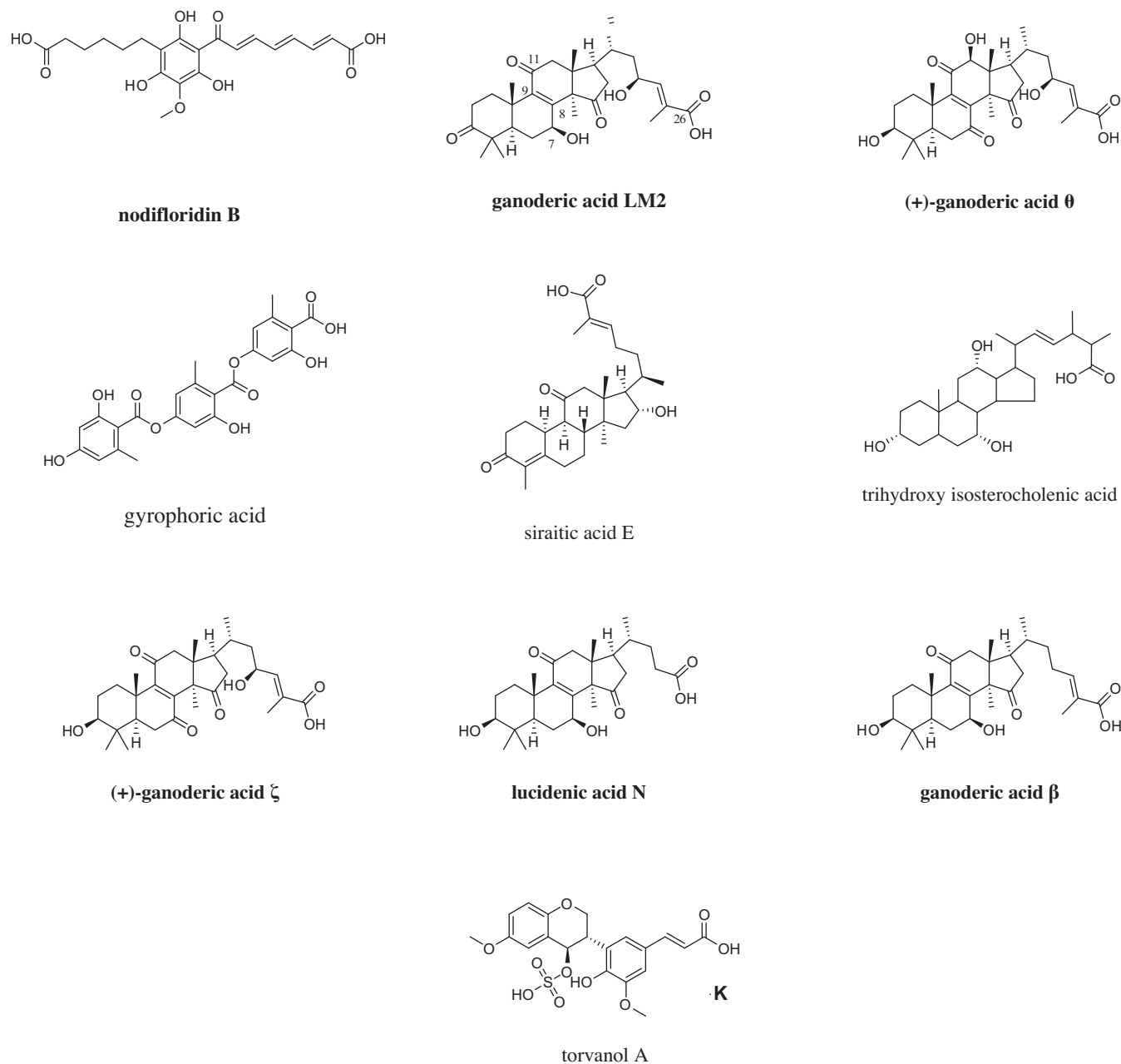
nodifloridin B

ganoderic acid LM2

(+)-ganoderic acid θ

gyrophoric acid

siraitic acid E

trihydroxy isosterocholenic acid

(+)-ganoderic acid ζ

lucidenic acid N

ganoderic acid β

torvanol A

Chart 4. VHs resulting from the virtual screening of the 3bej-1-s pharmacophore model: 5 of 10 VHs are constituents from *G. lucidum* (bold names).

validated in part I of this study,[42] were applied using the software LigandScout.[47] These models, covering diverse FXR ligands with different binding modes, represent helpful tools for pharmacophore profiling of the investigated 25 *Ganoderma* constituents (Table 2).

The profiling results, which were performed in a rigid fitting mode, show that the highest number of *Ganoderma* constituents can be identified by virtual screening with the 3bej-2 model, as the underlying PDB entry 3bej comprises a steroidal ligand. In comparison to the 3bej-1s model (Fig. 3), the chemical features on the side chain have been deleted and the ionic interaction with Arg331 is represented by a hydrogen bond acceptor instead of a negatively ionizable feature (Fig. 8). However, despite the significant generalization resulting from this modification, 3bej-2 still was not able to find all FXR-active compounds, which might be explained by the applied rigid fitting mode and the defined conformation of the structures. In flexible fitting mode all FXR-active compounds from *G. lucidum* except for compound **2** were found.

This can be explained by the lack of a hydrogen bond accepting group in compound **2** that could map the feature towards His447, near position 17. Remarkably, this His447 interaction is only present in the 3bej-based models. Obviously this interaction is not crucial for FXR agonism. At the same time, 3bej-2 has been shown to be the best predictive model for the triperpene compounds. The model could therefore be optimized in terms of making the hydrogen bond acceptor towards His447 an optional feature, which, however, would loosen significantly the model's restrictiveness in the virtual screening filtering experiment. As negative control for the application of the 3bej-2 model, the FXR-inactive group of fatty acid derivatives, that is, **5**, **6**, and **7** was neither found by a rigid nor by a flexible screening mode.

In order to get deeper structural insights into triterpenoid-mediated FXR activation, the most active compounds **2** and **13** were docked into the FXR ligand binding domain. The PDB entry 3bej[44] was selected as 3D representation of the FXR binding pocket
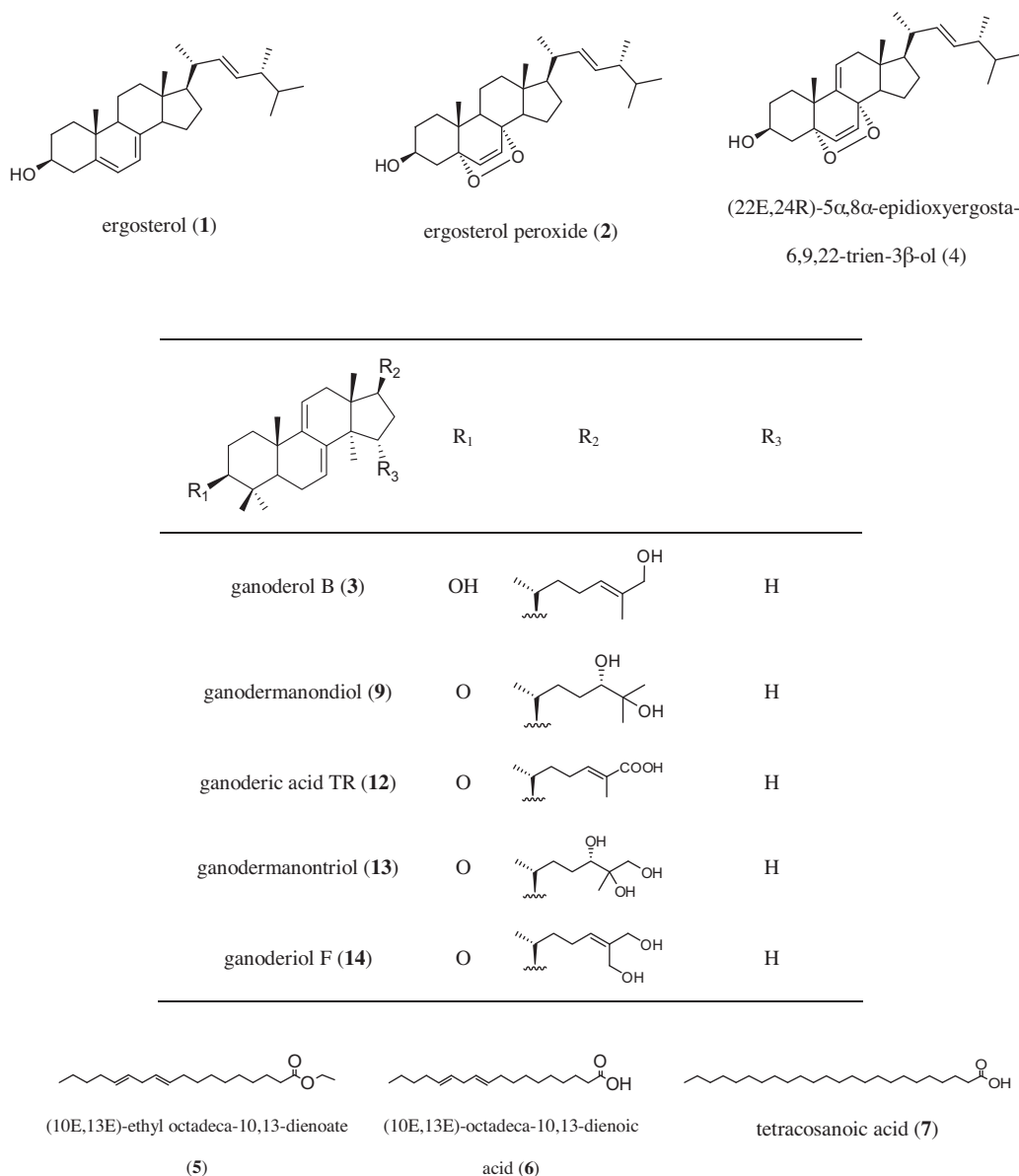
ergosterol (**1**)

ergosterol peroxide (**2**)

(22E,24R)-5α,8α-epidioxyergosta-

6,9,22-trien-3β-ol (4)

	R₁	R₂	R₃
ganoderol B (**3**)	OH	(structure, OH)	H
ganodermanondiol (**9**)	O	(structure, OH, OH)	H
ganoderic acid TR (**12**)	O	(structure, COOH)	H
ganodermanontriol (**13**)	O	(structure, OH, OH, OH)	H
ganoderiol F (**14**)	O	(structure, OH, OH)	H

(10E,13E)-ethyl octadeca-10,13-dienoate

(**5**)

(10E,13E)-octadeca-10,13-dienoic

acid (**6**)

tetracosanoic acid (**7**)

Chart 5. Chemical structures of tested *G. lucidum* substances.

because it accommodates a steroidal ligand, which is surmised to best reflect the FXR receptor conformation when bound to a triterpene ligand (Fig. 8). Among the predicted binding poses, two distinct binding orientations of the steroid ring were observed: The positioning of **2** was similar to the experimentally determined binding mode of MFA-1 in 3bej. In contrast, a flipped orientation was observed for compound **13**. Interestingly, this binding mode corresponds to the 6-ECDCA orientation within the rat FXR binding site determined by X-ray crystallography (PDB entry 1osv[48]) and was also in line with SAR studies on bile alcohols as FXR ligands by Iguchi et al.[49] In both docked ligand orientations, interactions with Arg331 via hydrogen bonds were observed (Fig. 9). All other contacts to the non-polar binding pocket were established via hydrophobic groups.

3. Conclusions

For the target-oriented selection of natural products and their constituents interacting with FXR we used a combination of pharmacophore-based virtual screening and experimental validation of multi-component mixtures. Accordingly, the heuristic assumption

of FXR-inducing lanostane-type triterpenes from *G. lucidum* together with the positively tested extracts of this TCM mushroom prompted us to investigate 25 *Ganoderma* constituents. Five lanostanes were identified as distinct FXR-inducing natural compounds. An FXR agonistic activity of these compounds was confirmed using two independent approaches, that is, a promoter–reporter study and analysis of the mRNA levels of the FXR-regulated gene CYP7A1. Additionally, the inhibition of TNF or LPS induced expression of IL-8 and *E*-selectin in human endothelial cells proposes these compounds as constituents of *G. lucidum* accountable for its anti-inflammatory effect. These mechanisms may involve the regulation of the nuclear receptor FXR by these compounds.

The applied in silico approach provided us with a targeted selection of promising natural starting material by correctly predicting the novel FXR-inducing chemical class of lanostane-type triterpenes. Investigation of the putative binding mode by molecular docking studies of the most active compounds ergosterol peroxide (**2**) and ganodermanontriol (**13**) enabled insight into the binding mode, which revealed crucial hydrogen bond interactions between the contemplated structure and Arg331 of the nuclear receptor backbone.
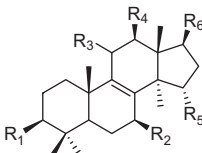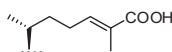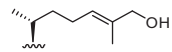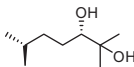
6786

U. Grienke et al./Bioorg. Med. Chem. 19 (2011) 6779–6791
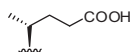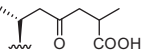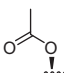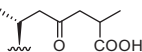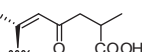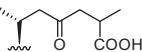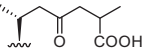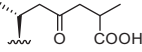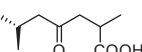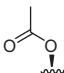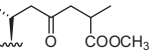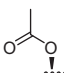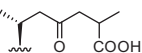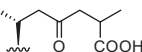
	R₁	R₂	R₃	R₄	R₅	R₆
ganoderic acid DM (**8**)	O	O	H	H	H	
ganoderon B (**10**)	OH	O	H	H	H	
lucidumol A (**11**)	O	O	H	H	H	
lucidenic acid A (**15**)	O	OH	O	H	O	
ganoderic acid D (**16**)	O	OH	O	H	O	
ganoderic acid F (**17**)	O	O	O		O	
ganoderenic acid D (**18**)	O	OH	O	H	O	
ganoderic acid J (**19**)	O	O	O	H	OH	
ganoderic acid B (**20**)	OH	OH	O	H	O	
ganoderic acid A (**21**)	O	OH	O	H	OH	
12β-hydroxy-3,7,11,15,23-pentaoxo-5α-lanost-8-en-26-oic acid (**22**)	O	O	O	O	O	
methyl ganoderate H (**23**)	OH	O	O		O	
ganoderic acid H (**24**)	OH	O	O		O	
ganoderic acid AM1 (**25**)	OH	O	O	H	O	

Chart 5. (*continued*)

4. Experimental

4.1. Virtual Chinese Herbal Medicine (CHM) database

The molecular 3D database CHM used in this study has been generated previously.[43] It comprises 10,216 compounds, which are related to natural products used in traditional Chinese medicine. The 3D structures of the compounds were built and consequently energetically minimized using the structure editor of Catalyst (www.accelrys.com). The ConFirm algorithm was applied to create conformational models for the compounds using the following settings: maximum number of conformers = 100,

generation type = fast quality, and energy range = 20 kcal/mol above the calculated lowest energy conformation.[43]

4.2. Model generation for a pharmacophore-based virtual screening

The two ligand-receptor complexes used for pharmacophore creation are accessible via the PDB with the accession codes 1osh and 3bej,[44] respectively. Models based on these PDB entries were generated using LigandScout software.[47] The resulting models were exported into DiscoveryStudio (www.accelrys.com) for optimization and virtual screening. For each model, one version
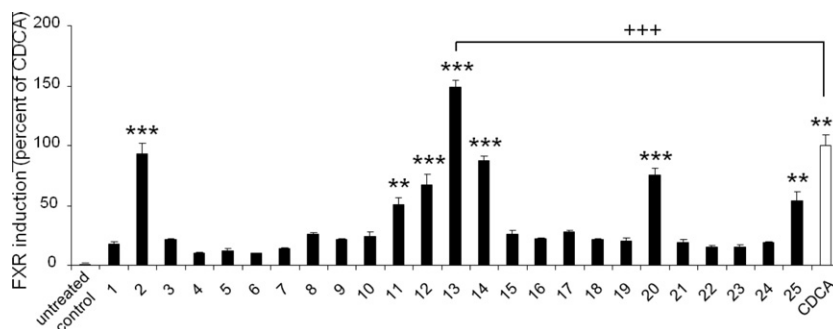
Figure 4. Induction of FXR-dependent transcription by *G. lucidum* constituents (compounds **1–25**, 10 µM each). The data (mean values ± SEM, *n* = 4–8) were normalized for renilla luciferase activity. The results are expressed as the difference in firefly luciferase activity between control and stimulated cells, normalized to the effect of positive control (CDCA, 25 µM); (***p <0.001, **p <0.01, +++p <0.001, ANOVA, Bonferroni post-test)
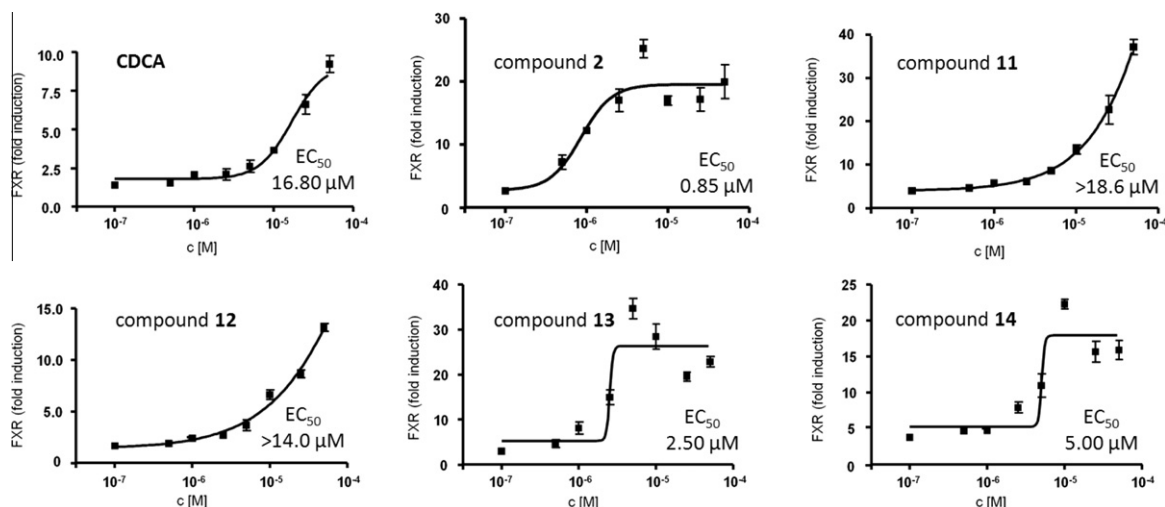

Figure 5. Dose-dependent activation of FXR reporter by selected *G. lucidum* constituents. Effects of indicated concentrations of compounds **2**, **11**, **12**, **13** and **14** on activity of FXR-driven luciferase reporter were determined as described in Figure 2. The data were normalized to expression of renilla luciferase (mean values ± SEM, *n* = 4–8). For **11** and **12** the exact EC_{50} values could not be determined since the induction did not reach saturation at maximal concentrations used in this experiment (50 µM). Very similar data were obtained in an independent experiment.
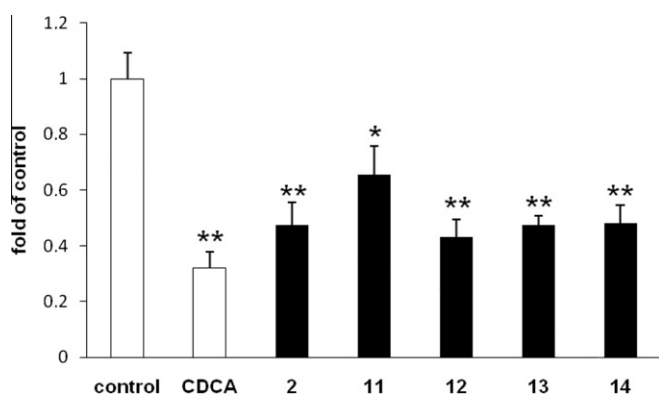

Figure 6. Expression of CYP7A1 mRNA. HepG2 cells treated with **2**, **12**, **13** and **14** (50 µM) for 6 h in DMEM containing 10% FCS; data expressed as fold of control cells treated with medium/0.1% DMSO; (*p <0.05, **p <0.01).

containing a shape (-*s*) restriction was generated using the bound ligand in the respective PDB complex entry.

4.3. Virtual screening of the *Ganoderma* compounds

The structures of all available isolated constituents from *G. lucidum* (**1–25**) were generated using ChemBioDraw Ultra 11.0. All compounds were exported as sd-files and submitted to conformational analysis using Discovery Studio 2.5 and the 'BEST' option. For each molecule, a maximum of 255 conformers within an energy range of 20 kcal/mol above the calculated energy minimum was allowed. The parallel mapping of the 25 compounds into FXR agonist pharmacophore models was performed using the 'Ligand Profiler' protocol of Discovery Studio with the 'BEST' fitting algorithm and a minimum inter-feature distance of 0.00001. All other parameters were kept as default.

4.4. Natural material and isolated pure compounds

The dried fruiting bodies of *G. lucidum* used for the preparation of extracts were purchased in Beijing, China. The quality was checked according to the monograph língzhī of the Chinese Pharmacopoeia. The fruit powder of *Capsicum annuum*, the dried leaves of *G. biloba*, the dried herb material of *R. graveolens*, and the dried fruits of *V. agnus-castus* were obtained from 'Mag. Kottas–Heilkräuter', Eitnergasse 8, 1230 Vienna, Austria. The dried roots of *R. graveolens* were supplied by 'Johann Strillinger–Gartenbau', Eiberg 8, 6306 Söll, Austria. The dried roots of *P. ginseng* were purchased from 'Mag. Stöger–Plantasia', Heinrich-Handel-Mazzetti-Platz, 5110 Oberndorf, Austria.

Voucher specimens (JR-20080605-A1, JR-20080429-A4, JR-20080429-A3, JR-20080429-A1, JR-20080429-A2, JR-20051
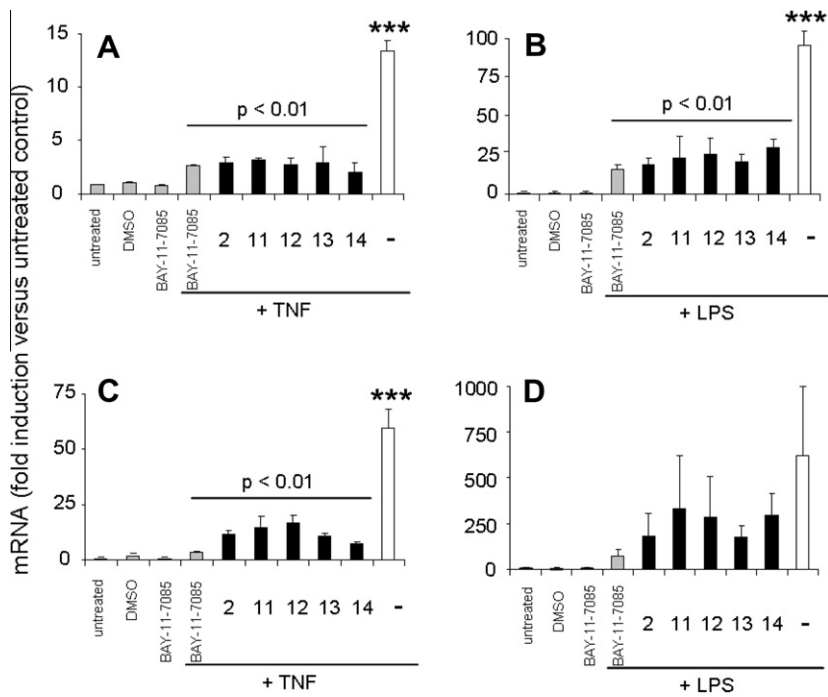
Figure 7. Anti-inflammatory effect of FXR inducing compounds from *G. lucidum* was determined in HUVEC as described in experimental section. The effect of compounds (5 µM) on TNF (100 ng/mL) or LPS (300 ng/mL) induced IL-8 (A, B) and *E*-Selectin (C, D) is expressed as fold induction of the respective mRNA expression in comparison with the untreated control; (***p <0.001, ANOVA, Bonferroni post-test).

Table 2
Pharmacophore profiling results of all models used in this study against the 25 tested *Ganoderma* constituents (+, VHs; −, virtual non-hits; *Ganoderma* compounds with experimentally determined FXR-inducing activity at 10 µM are highlighted in gray)

Models versus compds	1osh-1-s	1osh-1	1osh-2-s	1osh-2	3bej-1-s	3bej-1	3bej-2-s	3bej-2	3fli	3fli-s	3dct	3dct-s
1	−	−	−	−	−	−	−	−	−	−	−	−
2	−	−	−	−	−	−	−	−	−	−	−	−
3	−	−	−	−	−	−	−	+	−	−	−	−
4	−	−	−	−	−	−	−	−	−	−	−	−
5	−	+	−	−	−	−	−	−	+	+	−	−
6	−	+	−	−	−	−	−	−	+	+	−	−
7	−	+	−	−	−	−	−	−	+	+	−	−
8	−	−	−	−	−	−	+	+	−	−	−	−
9	−	−	−	−	−	−	+	+	−	−	−	−
10	−	−	−	−	−	−	−	+	−	−	−	−
11	−	−	−	−	−	−	−	−	−	−	−	−
12	−	−	−	−	−	−	−	−	−	−	−	−
13	−	−	−	−	−	−	+	+	−	−	−	−
14	−	−	−	−	−	−	−	+	−	−	−	−
15	−	−	−	−	−	−	−	−	−	−	−	−
16	−	−	−	−	−	−	−	−	−	−	−	−
17	−	−	−	−	−	−	−	−	−	−	−	−
18	−	−	−	−	−	−	−	−	−	−	−	−
19	−	−	−	−	−	−	−	−	−	−	−	−
20	−	−	−	−	−	−	−	+	−	−	−	−
21	−	−	−	−	−	−	−	−	−	−	−	−
22	−	−	−	−	−	−	−	−	−	−	−	−
23	−	−	−	−	−	−	−	+	−	−	−	−
24	−	−	−	−	−	−	−	−	−	−	−	−
25	−	−	−	−	−	−	−	+	−	−	−	−

009-A1, JR-20091203-D1) are deposited in the Herbarium of the Institute of Pharmacy/Pharmacognosy, University of Innsbruck, Austria.

Dichloromethane (DCM) and methanolic (MeOH) extracts were produced from the six selected natural materials. In a preliminary step 1 g of each drug was chopped and subsequently extracted for 15 min with 10 mL DCM in an ultrasonic bath. After centrifugation

the supernatant was evaporated under reduced pressure and the acquired DCM crude extract was collected. After drying of the remaining drug material a methanolic crude extract was then obtained by the same procedure as described above.

For the preparation of the enriched ethyl acetate (EA) fraction of *V. agnus-castus*, 200 g ground fruits were subjected to a Soxhlet extraction with 70% ethanol as a solvent. After four days the
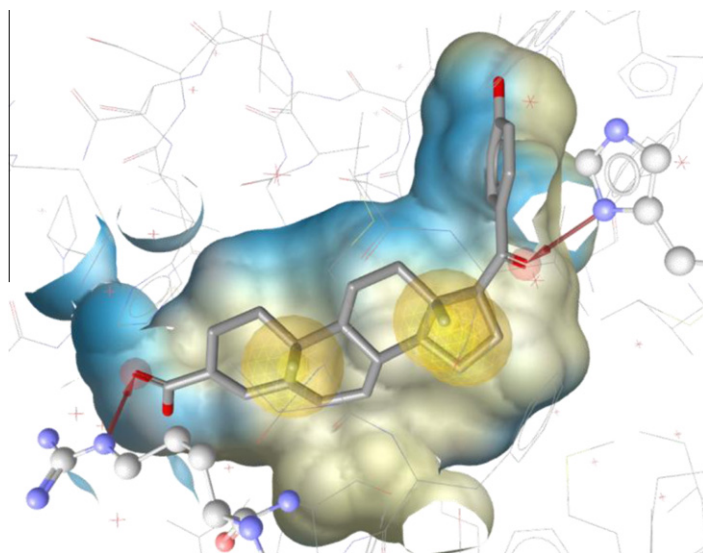
Figure 8. Best fitting FXR pharmacophore model (3bej-2) for investigated *Ganoderma* constituents. Crucial interactions of the ligand (MFA-1) with Arg331 and His447 are highlighted in ball-and-stick style.
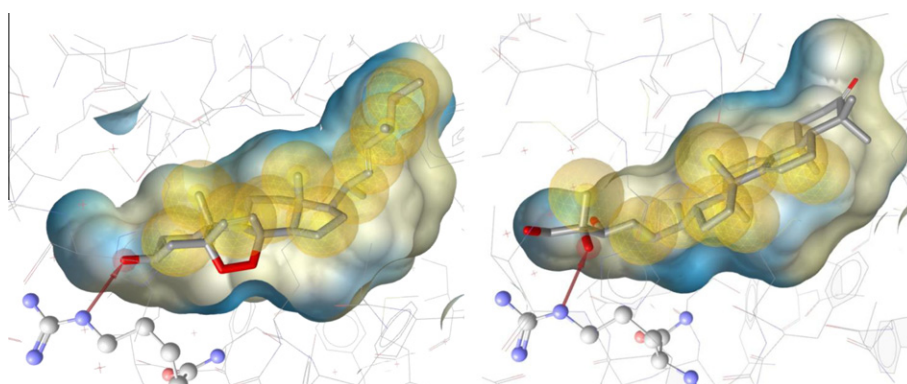

Figure 9. Predicted interactions of **2** and **13** with the Arg331 residue of the FXR protein backbone via hydrogen bonds.

obtained ethanolic extract (28.43 g) was suspended in water and subsequently partitioned between *n*-hexane (4 × 200 mL) and EA (3 × 200 mL). The EA fraction was investigated by LC–MS and proved to be enriched with virtually predicted flavonoids.

Extraction and isolation procedure of the *Ganoderma* constituents **1**–**25** as well as their physico-chemical properties were described previously.[45,46,50–53] The purity of these compounds was determined by HPLC and NMR to be ⩾ 98%.

Dihydrocapsaicin (declared purity approx. 90%) was purchased from Sigma–Aldrich (St. Louis, MO).

4.5. Cell culture, plasmids, and reagents

Human embryonic kidney-293 cells (HEK-293) from American Type Culture Collection (Manassas, VA, USA) were grown in Dulbecco's Modified Eagle's Medium (DMEM) (Sigma, St. Louis, MO) supplemented with 10% fetal bovine serum (FBS), penicillin/streptomycin, and 1% L-glutamine. TERT technology (hTERT) immortalized human umbilical vein cells (HUVECtert)[54] were cultured in M199 Medium (Sigma–Aldrich, St. Louis, MO) supplemented with 20% FBS, endothelial cell growth supplement (Technoclone, Austria) and antibiotics. The luciferase reporter plasmid (ECRE)5TK-Luc, the expression vector for mouse FXR, the expression vector for mouse RXR were kindly provided by Profes-

sor Glass CK (UCSD, La Jolla, CA). The vector pSV40-renillaLuc was obtained from Promega (Madison, WI, USA), the pcDNA3.1 from Invitrogen (Carlsbad, CA, USA). DMSO, CDCA and LPS (*Escherichia coli* 055:B5) were purchased from Sigma–Aldrich (St. Louis, MO), human recombinant TNFα was obtained from Peprotech (Rocky Hill, NJ).

4.6. Reporter gene assay for FXR activation

Activation of FXR was tested in HEK-293 cells seeded in 48 well plates (NUNC) and transiently transfected with the elements of the FXR reporter assay system (total DNA 0.3 ng/well). The firefly luciferase reporter containing quintuple RXR:FXR binding site and the respective expression plasmids for full length murine FXR and RXRα were introduced by transient transfection performed with the calcium phosphate technique. For monitoring transfection efficiency pSV40-renillaLuc was cotransfected. To normalize the amount of DNA transfected, pcDNA3.1 vector was added where appropriate. Cells were stimulated for 18 h with vehicle (DMSO) or with ligands at concentrations as indicated. Luciferase activity was determined from the cell lysates using Dual-Luciferase Kit (Promega, Madison, WI, USA), measured with Victor2 multilabel counter (Wallac, Finland). The firefly luciferase values were normalized with the renilla luciferase value measured for the

respective sample (relative luciferase units). FXR induction was determined as measurement of three independent experiments performed in quadruplicates and expressed as percent induction (mean values ± SEM) compared with the FXR ligand CDCA used as a reference in each respective experiment. Statistical significance of FXR induction was assessed by ANOVA-multiple comparison with Bonferroni post-test, whereby *p* values of less than 0.05 were regarded as statistically significant. The EC_{50} values were calculated by non-linear regression analysis using the equation for the sigmoidal dose response of GraphPad Prism 4.0 (GraphPad Software Inc., La Jolla, CA).

4.7. Inhibition of expression of inflammatory mediators and cell adhesion molecules

Monolayers of subconfluent quiescent HUVECtert cells were pre-treated for 10 min with the plant material or inhibitor as indicated, followed by stimulation with 100 ng/mL of TNFα (Pepro-Tech, Rocky Hill, NJ) or 300 ng/mL of LPS (Sigma–Aldrich, St. Louis, MO) for 30 min or 4 h, respectively. RNA was extracted from the cells using QIAzol lysis reagent (Qiagen, Hilden, Germany), 900 ng of RNA was reverse transcribed with MulV-RT using Oligo d(T) primers (Applied Biosystems, Carlsbad, CA). Relative expression of the genes of interest was determined by Q-PCR (Roche, Basel, Switzerland). Primers were designed with PRIMER3 software from the Whitehead Institute for Biomedical Research (Cambridge, MA) using the reference mRNA sequences of respective genes from the GeneBank (www.ncbi.nlm.nih.gov). For inteleukin-8 primers 5′-ctcttggcagccttcctgatt-3′(forward) and 5′-tatgcactgacatctaagttct ttagca-3′(reverse), for *E*-selectin 5′-ggtttggtgaggtctgctc-3′(forward) and 5′-tgatctgtcccggaactgc-3′(reverse) were used. Relative quantification of the investigated genes was calculated by normalization to a housekeeping gene β2-microglobulin using the mathematical model by Pfaffl,[55] and presented as fold variation over the control.

4.8. Analysis of expression of FXR downstream genes by qPCR

HepG2 cells were grown in 24-well dishes (NUNC) in DMEM supplemented with antibiotics (100 U/mL penicillin, 100 μg/mL streptomycin, 25 μg/mL amphotericin B), 1% glutamine and 10% FBS. The cells were stimulated in the same medium with the analyzed compounds or positive control (chenodeoxycholic acid, CDCA) dissolved in DMSO (final concentration 0.1%) at a concentration of 50 μM for 6 h. The incubation was terminated and RNA was isolated using TriFast reagent (PeqLab, Erlangen, Germany). A Gene-Amp RNA-PCR kit and oligo d(T)16 primers (Applied Biosystems, Foster City, CA) were used for cDNA synthesis from 900 ng of total RNA. Quantitative real-time PCR (qPCR) was performed using the Step One Plus (Applied Biosystems), FastStart SYBR Green Master Mix (Roche Diagnostics, Indianapolis, IN), and specific primers for amplification of CYP7A1 (Qiagen, Venlo, The Netherlands). CYP7A1 expression was normalized to the expression levels of β2-microglobulin using primers obtained from the same company.

4.9. Computational docking

Computational docking experiments were performed using GOLD 3.1 (www.ccdc.cam.ac.uk/products/life_sciences/gold/) with default settings. Protein and ligand preparations for docking were performed within GOLD.

Acknowledgments

Supplementary data

Supplementary data associated with this article can be found, in the online version, at doi:10.1016/j.bmc.2011.09.039. These data include MOL files and InChiKeys of the most important compounds described in this article.

References and notes

1. Forman, B. M.; Goode, E.; Chen, J.; Oro, A. E.; Bradley, D. J.; Perlmann, T.; Noonan, D. J.; Burka, L. T.; McMorris, T.; Lamph, W. W.; Evans, R. M.; Weinberger, C. *Cell* **1995**, *81*, 687.
2. Fiorucci, S.; Rizzo, G.; Donini, A.; Distrutti, E.; Santucci, L. *Trends Mol. Med.* **2007**, *13*, 298.
3. Pellicciari, R.; Costantino, G.; Fiorucci, S. *J. Med. Chem.* **2005**, *48*, 5383.
4. Shen, H.; Zhang, Y.; Ding, H.; Wang, X.; Chen, L.; Jiang, H.; Shen, X. *Cell. Physiol. Biochem.* **2008**, *22*, 1.
5. Makishima, M.; Okamoto, A. Y.; Repa, J. J.; Tu, H.; Learned, R. M.; Luk, A.; Hull, M. V.; Lustig, K. D.; Mangelsdorf, D. J.; Shan, B. *Science* **1999**, *284*, 1362.
6. Parks, D. J.; Blanchard, S. G.; Bledsoe, R. K.; Chandra, G.; Consler, T. G.; Kliewer, S. A.; Stimmel, J. B.; Willson, T. M.; Zavacki, A. M.; Moore, D. D.; Lehmann, J. M. *Science* **1999**, *284*, 1365.
7. Wang, H.; Chen, J.; Hollister, K.; Sowers, L. C.; Forman, B. M. *Mol. Cell* **1999**, *3*, 543.
8. Goodwin, B.; Jones, S. A.; Price, R. R.; Watson, M. A.; McKee, D. D.; Moore, L. B.; Galardi, C.; Wilson, J. G.; Lewis, M. C.; Roth, M. E.; Maloney, P. R.; Willson, T. M.; Kliewer, S. A. *Mol. Cell* **2000**, *6*, 517.
9. Lu, T. T.; Makishima, M.; Repa, J. J.; Schoonjans, K.; Kerr, T. A.; Auwerx, J.; Mangelsdorf, D. J. *Mol. Cell* **2000**, *6*, 507.
10. Lew, J.-L.; Zhao, A.; Yu, J.; Huang, L.; de Pedro, N.; Pelaez, F.; Wright, S. D.; Cui, J. *J. Biol. Chem.* **2004**, *279*, 8856.
11. Willson, T. M.; Jones, S. A.; Moore, J. T.; Kliewer, S. A. *Med. Res. Rev.* **2001**, *21*, 513.
12. Pellicciari, R.; Fiorucci, S.; Camaioni, E.; Clerici, C.; Costantino, G.; Maloney, P. R.; Morelli, A.; Parks, D. J.; Willson, T. M. *J. Med. Chem.* **2002**, *45*, 3569.
13. Maloney, P. R.; Parks, D. J.; Haffner, C. D.; Fivush, A. M.; Chandra, G.; Plunket, K. D.; Creech, K. L.; Moore, L. B.; Wilson, J. G.; Lewis, M. C.; Jones, S. A.; Willson, T. M. *J. Med. Chem.* **2000**, *43*, 2971.
14. Dussault, I.; Beard, R.; Lin, M.; Hollister, K.; Chen, J.; Xiao, J.-H.; Chandraratna, R.; Forman, B. M. *J. Biol. Chem.* **2003**, *278*, 7027.
15. www.clinicaltrials.gov, accessed August 25, 2011.
16. Akwabi-Ameyaw, A.; Bass, J. Y.; Caldwell, R. D.; Caravella, J. A.; Chen, L.; Creech, K. L.; Deaton, D. N.; Madauss, K. P.; Marr, H. B.; McFadyen, R. B.; Miller, A. B.; Navas, F.; Parks, D. J.; Spearing, P. K.; Todd, D.; Williams, S. P.; Bruce Wisely, G. *Bioorg. Med. Chem. Lett.* **2009**, *19*, 4733.
17. Feng, S.; Yang, M.; Zhang, Z.; Wang, Z.; Hong, D.; Richter, H.; Benson, G. M.; Bleicher, K.; Grether, U.; Martin, R. E.; Plancher, J.-M.; Kuhn, B.; Rudolph, M. G.; Chen, L. *Bioorg. Med. Chem. Lett.* **2009**, *19*, 2595.
18. Abel, U.; Schlueter, T.; Schulz, A.; Hambruch, E.; Steeneck, C.; Hornberger, M.; Hoffmann, T.; Perovic-Ottstadt, S.; Kinzel, O.; Burnet, M.; Deuschle, U.; Kremoser, C. *Bioorg. Med. Chem. Lett.* **2010**, *20*, 4911.
19. Richter, H. G. F.; Benson, G. M.; Blum, D.; Chaput, E.; Feng, S.; Gardes, C.; Grether, U.; Hartman, P.; Kuhn, B.; Martin, R. E.; Plancher, J.-M.; Rudolph, M. G.; Schuler, F.; Taylor, S.; Bleicher, K. H. *Bioorg. Med. Chem. Lett.* **2011**, *21*, 191.
20. Flatt, B.; Martin, R.; Wang, T.-L.; Mahaney, P.; Murphy, B.; Gu, X.-H.; Foster, P.; Li, J.; Pircher, P.; Petrowski, M.; Schulman, I.; Westin, S.; Wrobel, J.; Yan, G.; Bischoff, E.; Daige, C.; Mohan, R. *J. Med. Chem.* **2009**, *52*, 904.
21. Mencarelli, A.; Fiorucci, S. *J. Cell Mol. Med.* **2010**, *14*, 79.
22. Fiorucci, S.; Cipriani, S.; Mencarelli, A.; Renga, B.; Distrutti, E.; Baldelli, F. *Curr. Mol. Med.* **2010**, *10*, 579.
23. Lundquist, J. T.; Harnish, D. C.; Kim, C. Y.; Mehlmann, J. F.; Unwalla, R. J.; Phipps, K. M.; Crawley, M. L.; Commons, T.; Green, D. M.; Xu, W.; Hum, W. T.; Eta, J. E.; Feingold, I.; Patel, V.; Evans, M. J.; Lai, K.; Borges-Marcucci, L.; Mahaney, P. E.; Wrobel, J. E. *J. Med. Chem.* **2010**, *53*, 1774.
24. Gadaleta, R. M.; van Mil, S. W. C.; Oldenburg, B.; Siersema, P. D.; Klomp, L. W. J.; van Erpecum, K. J. *Biochim. Biophys. Acta, Mol. Cell Biol. Lipids* **2010**, *1801*, 683.
25. Lin, H.-R.; Abraham Donald, J. *Bioorg. Med. Chem. Lett.* **2006**, *16*, 4178.
26. Tobin, J. F.; Freedman, L. P. *Trends Endocrinol. Metab.* **2006**, *17*, 284.
27. Huang, T. H.-W.; Teoh, A. W.; Lin, B.-L.; Lin, D. S.-H.; Roufogalis, B. *Pharmacol. Res.* **2009**, *60*, 195.
28. Wu, J.; Xia, C.; Meier, J.; Li, S.; Hu, X.; Lala, D. S. *Mol. Endocrinol.* **2002**, *16*, 1590.
29. Urizar, N. L.; Liverman, A. B.; Dodds, D. N. T.; Silva, F. V.; Ordentlich, P.; Yan, Y.; Gonzalez, F. J.; Heyman, R. A.; Mangelsdorf, D. J.; Moore, D. D. *Science* **2002**, *296*, 1703.
30. Deng, R.; Yang, D.; Radke, A.; Yang, J.; Yan, B. *J. Pharmacol. Exp. Ther.* **2007**, *320*, 1153.
31. Brobst, D. E.; Ding, X.; Creech, K. L.; Goodwin, B.; Kelley, B.; Staudinger, J. L. *J. Pharmacol. Exp. Ther.* **2004**, *310*, 528.

32. Burris, T. P.; Montrose, C.; Houck, K. A.; Osborne, H. E.; Bocchinfuso, W. P.; Yaden, B. C.; Cheng, C. C.; Zink, R. W.; Barr, R. J.; Hepler, C. D.; Krishnan, V.; Bullock, H. A.; Burris, L. L.; Galvin, R. J.; Bramlett, K.; Stayrook, K. R. *Mol. Pharmacol.* **2005**, *67*, 948.
33. Lv, N.; Song, M. Y.; Kim, E. K.; Park, J. W.; Kwon, K. B.; Park, B. H. *Mol. Cell Endocrinol.* **2008**, *289*, 49.
34. Nam, S.-J.; Ko, H.; Ju, M. K.; Hwang, H.; Chin, J.; Ham, J.; Lee, B.; Lee, J.; Won, D. H.; Choi, H.; Ko, J.; Shin, K.; Oh, T.; Kim, S.; Rho, J.-R.; Kang, H. *J. Nat. Prod.* **2007**, *70*, 1691.
35. Ji, W.; Gong, B. Q. *J. Ethnopharmacol.* **2008**, *119*, 291.
36. Nozawa, H. *Biochem. Biophys. Res. Commun.* **2005**, *336*, 754.
37. Ji, W.; Gong, B. Q. *J. Ethnopharmacol.* **2007**, *113*, 318.
38. Sanodiya, B. S.; Thakur, G. S.; Baghel, R. K.; Prasad, G. B.; Bisen, P. S. *Curr. Pharm. Biotechnol.* **2009**, *10*, 717.
39. Paterson, R.; Russell, M. *Phytochemistry* **2006** *67*, 1985.
40. Berman, H.; Henrick, K.; Nakamura, H. *Nat. Struct. Mol. Biol.* **2003**, *10*, 980.
41. Downes, M.; Verdecia, M. A.; Roecker, A. J.; Hughes, R.; Hogenesch, J. B.; Kast-Woelbern, H. R.; Bowman, M. E.; Ferrer, J. L.; Anisfeld, A. M.; Edwards, P. A.; Rosenfeld, J. M.; Alvarez, J. G.; Noel, J. P.; Nicolaou, K. C.; Evans, R. M. *Mol. Cell* **2003**, *11*, 1079.
42. Schuster, D.; Markt, P.; Grienke, U.; Mihály-Bison, J.; Binder, M.; Noha, S. M.; Rollinger, J. M.; Stuppner, H.; Bochkov, V. N.; Wolber, G. *Bioorg. Med. Chem* **2011**, doi:10.1016/j.bmc.2011.09.056.

43. Fakhrudin, N.; Ladurner, A.; Atanasov, A. G.; Heiss, E. H.; Baumgartner, L.; Markt, P.; Schuster, D.; Ellmerer, E. P.; Wolber, G.; Rollinger, J. M.; Stuppner, H.; Dirsch, V. M. *Mol. Pharmacol.* **2010**, *77*, 559.
44. Soisson, S. M.; Parthasarathy, G.; Adams, A. D.; Sahoo, S.; Sitlani, A.; Sparrow, C.; Cui, J.; Becker, J. W. *Proc. Natl. Acad. Sci. U.S.A* **2008**, *105*, 5337.
45. Cheng, C.-R.; Yue, Q.-X.; Wu, Z.-Y.; Song, X.-Y.; Tao, S.-J.; Wu, X.-H.; Xu, P.-P.; Liu, X.; Guan, S.-H.; Guo, D.-A. *Phytochemistry* **2010**, *71*, 1579.
46. Yang, M.; Wang, X.; Guan, S.; Xia, J.; Sun, J.; Guo, H.; Guo, D.-A. *J. Am. Soc. Mass Spectrom.* **2007**, *18*, 927.
47. Wolber, G.; Langer, T. *J. Chem. Inf. Model.* **2005**, *45*, 160.
48. Mi, L. Z.; Devarakonda, S.; Harp, J. M.; Han, Q.; Pellicciari, R.; Willson, T. M.; Khorasanizadeh, S.; Rastinejad, F. *Mol. Cell* **2003**, *11*, 1093.
49. Iguchi, Y.; Kihira, K.; Nishimaki-Mogami, T.; Une, M. *Steroids* **2009**, *75*, 95.
50. Smith, W. B. *Org. Magn. Reson.* **1977**, *9*, 644.
51. Ma, W.; Li, X.; Wang, D.; Yang, C. *Yunnan Zhiwu Yanjiu* **1994**, *16*, 196.
52. Gauvin, A.; Smadja, J.; Aknin, M.; Faure, R.; Gaydou, E.-M. *Can. J. Chem.* **2000**, *78*, 986.
53. Wang, F. S.; Cai, H.; Yang, J. S.; Zhang, Y. M.; Hou, C. Y.; Liu, J. Q.; Zhao, M. J. *Yao Xue Xue Bao* **1997**, *32*, 447.
54. Chang, M. W.; Grillari, J.; Mayrhofer, C.; Fortschegger, K.; Allmaier, G.; Marzban, G.; Katinger, H.; Voglauer, R. *Exp. Cell Res.* **2005**, *309*, 121.
55. Kadl, A.; Huber, J.; Gruber, F.; Bochkov, V. N.; Binder, B. R.; Leitinger, N. *Vascul. Pharmacol.* **2002**, *38*, 219.